

# lncRNA LINC00284 promotes nucleus pulposus cell proliferation and ECM synthesis via regulation of the miR-205-3p/Wnt/ $\beta$ -catenin axis

MIN ZHU<sup>1,2</sup>, XIAOLING YAN<sup>3</sup>, YIN ZHAO<sup>4</sup>, HUAWEI XUE<sup>2</sup>, ZHEN WANG<sup>2</sup>,  
BO WU<sup>2</sup>, XIANGYANG LI<sup>2</sup> and YIXIN SHEN<sup>1</sup>

<sup>1</sup>Department of Spine Surgery, The Second Affiliated Hospital of Soochow University, Suzhou, Jiangsu 215004;

<sup>2</sup>Department of Spine Surgery, Nantong Third People's Hospital, Nantong, Jiangsu 226006;

<sup>3</sup>Chemotherapy Department, Affiliated Hospital of Nantong University, Nantong, Jiangsu 226001;

<sup>4</sup>Department of Spine Surgery, Shanghai Changzheng Hospital,  
The Second Military Medical University, Shanghai 200003, P.R. China

Received August 12, 2021; Accepted February 23, 2022

DOI: 10.3892/mmr.2022.12695

**Abstract.** Intervertebral disc degeneration (IDD) is a leading cause of degenerative spinal disease. Long non-coding RNA (lncRNA) LINC00284 is overexpressed in multiple types of cancer and promotes cancer cell proliferation and inhibits apoptosis; however, its role in human IDD and nucleus pulposus (NP) remain unclear. In the present study, intervertebral disc (IVD) tissues were collected from IDD patients for detection of LINC00284 expression using reverse transcription-quantitative PCR, the binding effect between miR-205-3p and LINC00284 was validated by dual-luciferase reporter assay. miR-205-3p and small interfering RNA (siRNA) was used for LINC00240 knockdown to investigate the proliferation, apoptosis of cells in the NP cells measured by Cell Counting Kit (CCK)-8 assay and Annexin V-FITC/Propidium Iodide (PI) staining with flow cytometry receptivity. IDD animal models were constructed for *in vivo* study of the role LINC00284 in IDD improvement. The results showed that LINC00284 expression was upregulated in IDD tissue and IL-1 $\beta$ -induced NP cells. LINC00284 knockdown resulted in an increase in IL-1 $\beta$ -induced NP cell proliferation, a decrease in apoptosis and matrix metalloproteinase-3 expression and an increase in expression of extracellular matrix (ECM) markers aggrecan and collagen II. *In vivo* experiments and histomorphometric analysis confirmed the protective effect of LINC00284 knockdown in IDD. LINC00284 was also shown to be a target of microRNA (miR)-205-3p, and

there was a negative correlation between LINC00284 and miR-205-3p levels in IDD tissue. Additionally, LINC00284 knockdown or miR-205-3p upregulation resulted in inhibition of Wnt/ $\beta$ -catenin signaling and subsequent degradation of the ECM. The present study demonstrated that LINC00284 activated the Wnt/ $\beta$ -catenin signaling via sponging miR-205-3p, resulting in inhibition of NP cell proliferation and ECM synthesis. These results suggested that targeting LINC00284 to rescue miR-205-3p expression may be a potential method for IDD management.

## Introduction

Intervertebral disc (IVD) degeneration (IDD) is major cause of degenerative spinal disease (1) and can lead to disability, heavy economic burden and a lower quality of life (2,3). Previous studies showed cellular and biochemical changes in IVD tissue in patients with IDD (4,5), including loss of living cells in the nucleus pulposus (NP) and destruction of extracellular matrix (ECM) in the IVD (6,7). Multiple biological approaches have been developed to prevent early IDD by promoting repair and regeneration of the ECM (8,9). Inflammation participates in the pathogenesis of ECM metabolism (7,10); proinflammatory cytokines inhibit ECM production in NP cells and increase levels of enzymes involved in ECM degradation, such as matrix metalloproteinases (MMPs) and a disintegrin and metalloproteinase with thrombospondin motifs (ADAMTS) (6,7). Additionally, the production of collagen and proteoglycan increases during disc degeneration (11,12). Therefore, inhibition of cell proliferation and repair of ECM synthesis dysfunction is a promising potential treatment strategy for IDD.

microRNAs (miRNAs or miRs) and long non-coding RNAs (lncRNAs) serve key roles in IDD production via regulation of proliferation or apoptosis of NP cells (13,14). Wan *et al* (15) investigated levels of lncRNAs in human IDD compared with normal NP tissue using lncRNA-mRNA microarrays and found that 67 lncRNAs were upregulated and 49 lncRNAs

---

*Correspondence to:* Dr Yixin Shen, Department of Spine Surgery, The Second Affiliated Hospital of Soochow University, 1055 Sanxiang Road, Suzhou, Jiangsu 215004, P.R. China  
E-mail: szdxsyx@163.com

**Key words:** intervertebral disc degeneration, long non-coding RNA LINC00284, microRNA-205-3p, Wnt/ $\beta$ -catenin signaling

were downregulated in IDD tissue (15). In addition to the lncRNAs identified by Wan *et al* (15), additional lncRNAs have been shown to be involved in progression of IDD, including lncRNA membrane associated guanylate kinase, WW and PDZ domain-containing 2 (MAG12) antisense RNA 3 (MAG12-AS3) (16) and lncRNA prostate androgen regulated transcript 1 (PART1) (17). LINC00284 has been reported as a potential target for management of ovarian and gastric cancer (18,19) due to its ability to promote cell proliferation and angiogenesis; however, its role in IDD remains unclear. The prevailing hypothesis holds that lncRNAs function as competing endogenous RNAs (ceRNAs) to sponge and regulate the availability of miRNAs (13). In previous studies, miR-205 has been reported to suppress proliferation of renal carcinoma cancer (20) and acute lymphoblastic leukemia cells (21). Chen *et al* (22) suggested that miR-205 accelerates ECM accumulation in mesangial cells; thus it is key to determine whether LINC00284 competitively binds with miR-205-3p to regulate proliferation of NP cells.

In NP cells, different signaling pathways associated with ECM metabolism are regulated by inflammation, such as the Wnt, NF- $\kappa$ B and ERK1/2 signaling pathways (8,23-25). Wnt signaling has been implicated in regulation of the inflammatory process in the musculoskeletal system (26,27), where it is involved in formation of tissue patterns during embryogenesis and carcinogenesis (28). Moreover, studies have shown that the Wnt signaling pathway is involved in pathogenesis of osteoarthritis and rheumatoid arthritis (29,30); however, the role of Wnt signaling in ECM metabolism in IDD remains unclear.

In the present study, the role and mechanisms of LINC00284 and miR-205-3p in IDD were investigated. It was hypothesized that LINC00284 possessed a potential binding site for miR-205-3p, which was detected using a dual luciferase reporter assay, and their interaction in cells of the NP was also investigated. Furthermore, the proliferation, apoptosis of NP cells as well as ECM synthesis were also investigated. Finally, a miR-205-3p/Wnt/ $\beta$ -catenin axis was also explored in proliferation of NP cells and in ECM synthesis mediated by LINC00284. In summary, the present study will provide a novel experimental and theoretical basis for targeted therapy of IDD.

## Materials and methods

**Human tissue samples.** Degenerated IVD tissue was collected from 30 patients (14 male, 16 female; median age, 62.3 years; age range, 51-71 years) with IDD and normal NP tissue was obtained from 30 patients (17 male, 13 female; median age, 40.6 years; age range, 32-49 years) with spinal cord injury between June 2018 and December 2020 at the Shanghai Changzheng Hospital (Shanghai, China). The collected tissues were rapidly frozen in liquid nitrogen and stored at  $-80^{\circ}\text{C}$ . The present study was approved by the Shanghai Changzheng Hospital (Shanghai, China), and followed the guidelines described in the Helsinki Declaration (31). Written informed consent was obtained for tissue sample collection from each participant.

**Cell culture and transfection.** Human NP cells were purchased from ScienCell Research Laboratories, Inc. (cat. no. 4800)

and cultured in NP Cell Medium (both ScienCell Research Laboratories, Inc.) at  $37^{\circ}\text{C}$  with 5%  $\text{CO}_2$  in a humidified incubator. NP cells had been initially isolated from NP of the human IVD; each vial contained  $>5 \times 10^5$  cells in 1 ml and NP cells were allowed to expand for 15 passages according to the manufacturer's instructions. Human embryonic kidney 293T cells (American Type Culture Collection; cat. no. CRL-1573) were cultured in DMEM containing 10% FBS (both Thermo Fisher Scientific, Inc.) at  $37^{\circ}\text{C}$  in a humidified incubator with 5%  $\text{CO}_2$ . LINC00284 specific small interfering (si)RNA (si-LINC00284) was used to knockdown LINC00284 expression and scramble siRNA was used as negative control (si-NC) and human miR-205-3p and scrambled miR-205-3p mimic (mi-NC) were transfected into cells at the concentration of  $20 \mu\text{M}$  using Lipofectamine<sup>®</sup> 3000 (Thermo Fisher Scientific, Inc.) at  $37^{\circ}\text{C}$  for 24 h according to manufacturer's instructions. All siRNAs, miRNA mimics and NCs were obtained from Shanghai GenePharma Co., Ltd. The sequences of constructs were as follows: si-LINC00284 sense, 5'-GCAUGUUAUUCACUAUUATT-3' and antisense, 5'-UAAUAGUGAAUUAACAUGCTT-3'; si-NC sense, 5'-GUUGAAUUAACUACACUUTT-3' and antisense, 5'-AAGUGUAAAGUUAUUCACCTT-3'; miR-205-3p mimic sense, 5'-GAUUUCAGUGGAGUGAAGUU-3' and antisense, 5'-AACUUCACUCCACUGAAAUC-3' and mi-NC sense, 5'-GGUAGUGCGGAAAGUUUAUU-3' and antisense, 5'-AAUAAACUUUCCGCACUACC-3'.

When cell confluence reached  $\sim 80\%$ , transfected NP cells were plated into 6- or 96-well plates at  $1 \times 10^5/\text{ml}$  for serum starvation overnight, then stimulated at  $37^{\circ}\text{C}$  using IL-1 $\beta$  (Prospec-Tany TechnoGene, Ltd.) at 5, 10 or 20 ng/ml for 24 h.

**Reverse transcription-quantitative (RT-q)PCR.** Total RNA was extracted from tissue or cells using TRIzol<sup>®</sup> (Thermo Fisher Scientific, Inc.). LINC00284, MMP-3, aggrecan and collagen II mRNA levels were detected using SYBR-Green qPCR kit (Takara Bio, Inc.) according to the protocol. Briefly the one-step RT-qPCR reaction was:  $10 \mu\text{l}$  of 2X One step TB Green RT-PCR Buffer III,  $0.4 \mu\text{l}$  of TaKaRa Ex Taq HS ( $5 \text{ U}/\mu\text{l}$ ),  $0.4 \mu\text{l}$  of PrimeScript RT enzyme Mix II,  $0.4 \mu\text{l}$  of forward primer ( $10 \mu\text{M}$ ),  $0.4 \mu\text{l}$  of reverse primer ( $10 \mu\text{M}$ ),  $2 \mu\text{l}$  of total RNA, and  $6 \mu\text{l}$  of RNase Free  $\text{dH}_2\text{O}$ , then subjected to reverse transcription for 5 min at  $42^{\circ}\text{C}$  and initially denatured at  $95^{\circ}\text{C}$  for 10 sec, and then to 40 cycles of amplification with the condition of  $95^{\circ}\text{C}$  denature for 5 sec, and  $60^{\circ}\text{C}$  annealing for 30 sec.  $\beta$ -actin was used as the housekeeping gene. The mature miR-205-3p expression levels in tissue and cells were detected using Hairpin-it<sup>™</sup> miRNA One-step qPCR-PCR SYBR Green kit (Shanghai GenePharma Co., Ltd.) according to the protocol. Briefly the reaction system was setup as:  $10 \mu\text{l}$  of One-Step SYBR Mix,  $0.5 \mu\text{l}$  of Enzyme Mix,  $0.5 \mu\text{l}$  of forward primer ( $2 \mu\text{M}$ ),  $0.4 \mu\text{l}$  of reverse primer ( $5 \mu\text{M}$ ),  $0.4 \mu\text{l}$  of ROX Reference Dye,  $2 \mu\text{l}$  of RNA template,  $6.2 \mu\text{l}$  of RNase Free  $\text{dH}_2\text{O}$ , then subjected to reverse transcription for 40 min at  $42^{\circ}\text{C}$  and initially denatured at  $94^{\circ}\text{C}$  for 3 min, and then to 40 cycles of amplification with the condition of:  $94^{\circ}\text{C}$  denature for 12 sec,  $62^{\circ}\text{C}$  annealing for 30 sec, and  $72^{\circ}\text{C}$  extension for 30 sec. Small U6 RNA was used as the endogenous control. RT-qPCR results were analyzed using the  $2^{-\Delta\Delta\text{Ct}}$  method (32). The primers were synthesized by Biomics Biotechnologies Co. Ltd. and the sequences are listed in Table I.

Table I. Primer sequences used for reverse transcription-quantitative PCR.

Name	Sequence, 5'→3'
LINC00284	F: TGTGGGTGCCAGGTTATGAC R: TGCGCTCATCTTCTCCTCAC
MMP-3	F: CTCTTCCTCAGGCGTGGAT R: AGGGAAACCTAGGGTGTGGA
Aggrecan	F: GATGATCTGGCAGGAGAAGGG R: CGTTTGTAGGTGGTGGCTGTG
Collagen II	F: CCGTGCTCCTGCCGTTT R: GACATCCTGGCCCTGACAC
β-actin	F: GCCGTTCCGAAAGTTGCCT R: ATCATCCATGGTGAGCTGGCG
miR-205-3p	F: CCTTCATTCCACCGGAGT R: GGTCCAGTTTTTTTTTTTTTTTTCAGA
U6 RNA	F: CTCGCTTCGGCAGCACA R: AACGCTTCACGAATTTGCGT

MMP, matrix metalloproteinase; miR, microRNA; F, forward; R, reverse.

**Western blot analysis.** The protein levels of MMP-3, aggrecan, collagen II and Wnt1, β-catenin and β-actin were detected using western blotting. Total proteins from IL-1β-treated cells were lysed in RIPA buffer with 1% PMSF and InStab™ Protease Cocktail (Shanghai Yeasen Biotechnology Co., Ltd.) and protein concentration was quantified using a Pierce BCA Protein Assay kit (Thermo Fisher Scientific, Inc.). Then, 20 μg/lane protein was resolved using 10% SDS-PAGE and transferred onto a PVDF membrane (MilliporeSigma), followed by blocking with EZ-Buffers N 1X BLOCK BSA in TBS (Sangon Biotech Co., Ltd.) for 2 h at room temperature. The blots were probed with the following antibodies (all 1:1,000; all from Abcam): Anti-MMP-3 (cat. no. ab52915), anti-collagen II (cat. no. ab188570), anti-aggrecan (cat. no. ab3778), anti-Wnt1 (cat. no. ab15251), anti-β-catenin (cat. no. ab223075) or anti-β-actin (cat. no. ab8226) at 4°C overnight, followed by incubation with horseradish peroxidase-conjugated goat anti-rabbit (cat. no. ab7090) for MMP-3, collagen II, Wnt1 and β-catenin detection or anti-mouse IgG (cat. no. ab47827) for aggrecan and β-actin for 1.5 h at room temperature. ECL Western Blotting Substrate (Thermo Fisher Scientific, Inc.) was used to visualize the signals. The mean gray values of blots were measured using ImageJ version 1.8.0 software (National Institutes of Health). β-actin was used for normalization.

**Cell proliferation assay.** Cell proliferation was detected using a Cell Counting Kit (CCK)-8 assay. After seeding into 96-well plates (5x10<sup>3</sup> cells/well) for 24 h, cells were transfected at 37°C with si-LINC00284, miR-205-3p mimics or NC for 24, 48 and 72 h. At 48 h post-transfection, 10 μl CCK-8 reagent (Abcam) was added per well and cells were incubated for 4 h at 37°C. The absorbance at 450 nm was measured. Untreated NP cells were used as the control.

**Cell apoptosis assay.** Annexin V-FITC/Propidium Iodide (PI) staining and flow cytometry analysis were used to detect NP cell apoptosis. At 48 h post-transfection, 1x10<sup>6</sup> cells/well were harvested, washed in PBS and plated in a 6-well plate. Annexin V-FITC Apoptosis Detection kit (MilliporeSigma) was used to measure cell apoptosis according to the manufacturer's instructions. Briefly, after washing with PBS twice, cells were resuspended in Annexin-V binding buffer, stained with the Annexin V-FITC/PI for 15 min at room temperature in the dark and analyzed using FACSCalibur and BD CellQuest™ Pro software version 6.0 (both BD Biosciences), and the apoptotic rate was calculated as the numbers of early + late apoptotic cells/total numbers of cell.

**Dual-luciferase reporter assay.** LINC00284 sponging of miR-205-3p was predicted using DIANA-LncBase V2 (carolina.imis.athena-innovation.gr) (33). The binding of LINC00284 with miR-205-3p was validated using dual-luciferase reporter assay. Wild-type (wt) or mutated (mut) LINC00284 sequence was constructed and inserted into a pGL3 vector (Promega Corporation) as luciferase reporter gene vectors. Briefly, 293T cells were cultured at 37°C overnight to 70-80% confluence, then ~2x10<sup>5</sup> cells were seeded into 24-well plates. After culturing at 37°C for 24 h, cells were co-transfected with wt-LINC00284 or mut-LINC00284 reporter vector and miR-205-3p mimics or mi-NC using Lipofectamine® 2000 (Thermo Fisher Scientific, Inc.) according to manufacturer's instructions. At 48 h post-transfection, luciferase reporter assay was performed using a Dual-Luciferase Reporter Assay System (Promega Corporation), the results were normalized with *Renilla* luciferase activity).

**IDD animal model construction.** To investigate the effect of LINC00284 in IDD *in vivo*, si-LINC00284 and si-NC were inserted into short hairpin (sh)RNA lentiviral vectors and packaged as sh-LINC00284 and sh-NC lentiviruses by Shanghai GenePharma Co., Ltd. A total of 24 male Sprague-Dawley rats (weight, 200-250 g; age, 3 months) were obtained from Nantong University (Nantong, China) for *in vivo* experiments and were housed under the condition of 18-26°C and 40-70% humidity, with a 12 h light/dark cycle and free access to food and water. The rats were randomly divided into three groups (n=8/group): sham, treated with sh-NC lentivirus (sham + sh-NC); IDD model, treated with sh-LINC00284 lentivirus (IDD + sh-LINC00284) and IDD NC, treated with sh-NC lentivirus treatment (IDD + sh-NC). All surgical procedures were performed as previously described (34). Briefly, to induce IDD, rats were anesthetized by intraperitoneal injection of pentobarbital sodium (40 mg/kg), then a midline longitudinal incision was made on the back. The left facet joint between the fourth and fifth lumbar (L4/5) vertebrae was removed to uncover the L4/5 IVD. Then, a 21-gauge needle was inserted into the IVD parallel to the endplate to a depth of 3 mm and held in place for 30 sec. The animal experiments were performed in accordance with the National Institutes of Health Guide for the Care and Use of Laboratory Animals (35) and were approved by the Animal Care and Use Committee of Nantong University (Nantong, China).

The lentivirus was injected into the anterior midline area of IVD 7 days after puncture using a microliter syringe with a 26-gauge needle (10 μl, Shanghai Gaoge Industry and Trade

Co., Ltd.) via the anterior transperitoneal midline, as previously described (36,37).

**X-ray and MRI examination.** At 7, 14 and 28 days after initial IVD puncture, six animals were randomly selected for X-ray and MRI examination. The animals were kept in a prone position with tails straightened on a molybdenum target radiographic image unit (GE Healthcare). IVD height was measured according to the disc height index (DHI) as previously described (38). DHI change (%) was calculated relative to sham + sh-NC group. Transverse relaxation time (T2) midsagittal MRI images were obtained via Siemens 3.0T Magneto Trio MRI System (Siemens Healthineers). T2 MRI images were analyzed by two independent radiologists blinded to the experimental conditions according to Pfirrmann MRI-grade system as previously described (39).

**Histological staining and morphological analysis.** IVD tissue was obtained following model rat sacrifice by intraperitoneal injection of sodium pentobarbital (100 mg/kg) 28 days after initial disc puncture. Tissue was fixed in 10% formalin for 48 h at room temperature, decalcified using 10% EDTA solution for 30 days at room temperature and embedded in paraffin wax. The paraffin blocks of IVD tissue were sectioned into 5  $\mu$ m coronal sections containing NP, annulus fibrosus (AF) and cartilaginous endplate. The sections were heated at 60°C for 30 min, and then dewaxed with xylene twice for 20 min each, and rehydration in descending alcohol series stained using a Hematoxylin-Eosin (H&E) Staining kit (Beijing Solarbio Science & Technology Co., Ltd.) or Modified Safranin O-Fast Green FCF Cartilage Stain kit (Beijing Solarbio Science & Technology Co., Ltd.) according to manufacturer's protocols. For histological grading, staining was categorized by two independent pathologists blinded to the experimental conditions on a scale of 4 (normal) to 12 points (severe degeneration) as described by Masuda *et al* (40) under a light microscope (Olympus CX43; Olympus Corporation; magnification, x100) and Olympus cellSens software version V3.2 (Olympus; Olympus Corporation) was used for analysis.

**Statistical analysis.** All data are presented as the mean  $\pm$  standard deviation of three independent experiments and were analyzed using SPSS version 19.0 (IBM Corp.). Differences between two groups were evaluated using unpaired Student's t-test; differences between  $\geq 3$  groups were compared using one-way ANOVA followed by post hoc Dunnett's or Tukey's. Spearman's rank correlation analysis was used to determine the correlation between LINC00284 and miR-205-3p expression.  $P < 0.05$  was considered to indicate a statistically significant difference.

## Results

**LINC00284 high expression in IDD tissue.** The expression levels of LINC00284 in IDD and normal tissue was evaluated using RT-qPCR. LINC00284 expression was significantly upregulated in 30 IDD samples compared with that in normal NP tissues (30 samples obtained from patients with spinal cord injury; Fig. 1). The results indicated that LINC00284 was overexpressed in NP tissues of IDD patients.

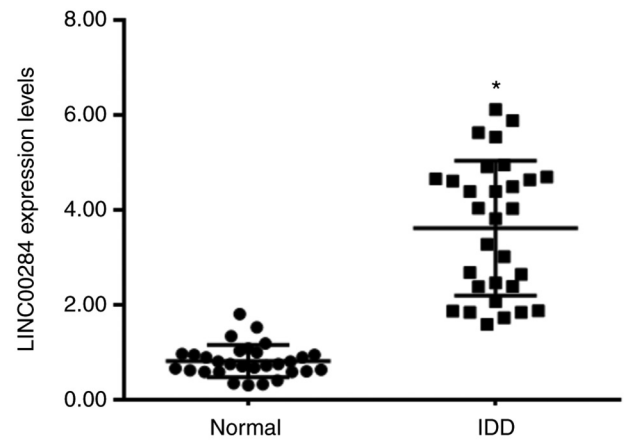


Figure 1. LINC00284 expression levels in 30 IDD and 30 normal tissue samples. IDD, intervertebral disc degeneration. \* $P < 0.001$  vs. normal tissue samples.

**LINC00284 expression increases in IL-1 $\beta$ -induced NP cells and promotes ECM degradation.** Human NP cells were treated with 5, 10 or 20-ng/ml IL-1 $\beta$  and LINC00284 expression was detected using RT-qPCR. LINC00284 expression was low in normal NP cells (control) but significantly increased following IL-1 $\beta$  treatment, with 5 ng/ml exerting the most significant increase (Fig. 2A). Thus, 5 ng/ml IL-1 $\beta$  was used in subsequent experiments.

To investigate whether IL-1 $\beta$  promotes IDD by stimulating NP cells and determine the role of LINC00284 in development of IDD, LINC00284 expression was knocked down using siRNA (Fig. 2B) and expression levels of MMP-3 and other ECM markers were measured using RT-qPCR and western blotting. IL-1 $\beta$  inhibited expression of aggrecan and collagen II but increased MMP-3 expression at both the mRNA and protein level. Additionally, in IL-1 $\beta$ -induced NP cells, LINC00284 knockdown decreased MMP-3 expression but increased aggrecan and collagen II expression levels compared with si-NC treated cells (Fig. 2C-I). The results indicated that LINC00240 may promote the development of IDD.

**LINC00284 knockdown promotes proliferation and inhibits apoptosis of IL-1 $\beta$ -induced NP cells.** To determine the role of LINC00284 in IDD, proliferation of IL-1 $\beta$ -induced NP cells following LINC00284 knockdown was detected using CCK-8 assay and Annexin V-FITC/PI staining with flow cytometry analysis. Compared with the control group, proliferation was inhibited in cells treated with 5 ng/ml IL-1 $\beta$  for 24, 48 and 72 h; however, in IL-1 $\beta$ -induced NP cells, si-LINC00284 promoted cell proliferation (Fig. 3A) but significantly decreased apoptosis (Fig. 3B and C), compared with si-NC-treated cells. The results indicated that LINC00240 may inhibit the proliferation, but promote the apoptosis, of NP cells in IDD patients.

**LINC00284 knockdown improves IDD in an animal model of IDD.** To evaluate the therapeutic effect of LINC00284 knockdown *in vivo*, intradiscal injection of sh-LINC00284 lentivirus was performed weekly in a needle puncture rat IDD model. Compared with 7 days after initial puncture, X-ray examination showed that IDD rats treated with sh-NC exhibited more

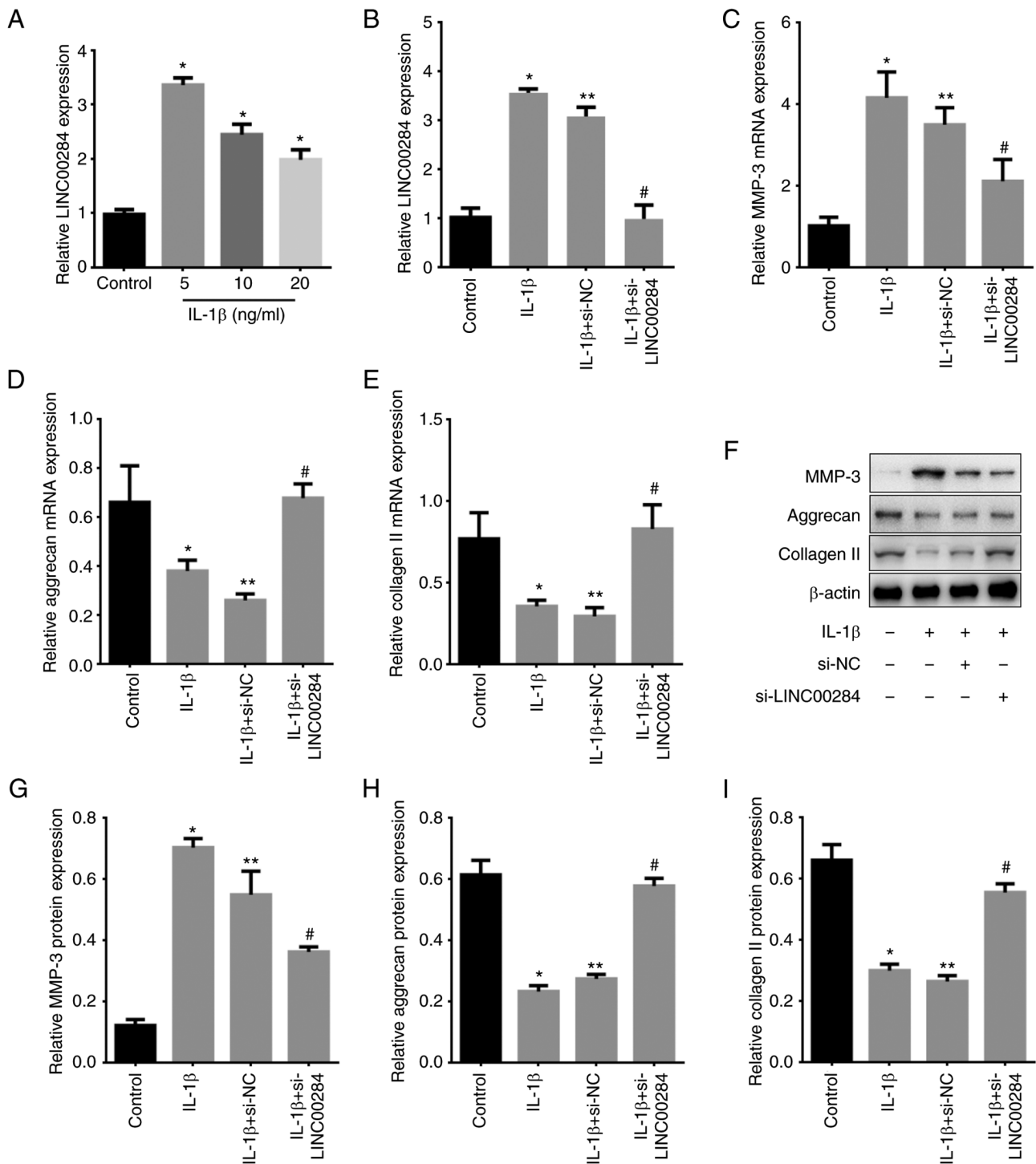


Figure 2. Expression of ECM markers is regulated by LINC00284 expression in IL-1 $\beta$ -induced NP cells. (A) LINC00284 expression following treatment with 5, 10 or 20 ng/ml IL-1 $\beta$ . (B) NP cells were transfected with si-LINC00284 to knock down LINC00284 expression. (C) MMP-3 mRNA levels were decreased by si-LINC00284 transfection. (D) Aggrecan and (E) collagen II mRNA levels were upregulated following si-LINC00284 transfection. (F) The blots of MMP-3, aggrecan and collagen II protein expression regulated by si-LINC00284 transfection in IL-1 $\beta$ -induced NP cells measured by western blot assay. (G) MMP-3, and ECM markers (H) aggrecan and (I) collagen II protein levels were regulated by si-LINC00284 transfection in IL-1 $\beta$ -induced NP cells. \*P<0.05 vs. Control; \*\*P<0.05 vs. IL-1 $\beta$ ; #P<0.05 vs. IL-1 $\beta$  + si-NC. ECM, extracellular matrix; si, small interfering; MMP-3, matrix metalloproteinase-3; NP, nucleus pulposus.

notable narrowing of disc height compared with sham rats treated with sh-NC on days 14 and 28. Following treatment of IDD rats with sh-LINC00284, the decline in disc height began to slow from days 7-28 (Fig. 4A) and the percentage DHI in the sh-LINC00284 group was 1.56, 1.28 and 1.32-fold higher than that in sh-NC IDD rats on days 7, 14 and 28, respectively (Fig. 4B). According to MRI examination, 14 and 28 days after

initial puncture, intradiscal injection with sh-NC in IDD rats exhibited weaker MRI signal than 7 days. Compared with sh-NC-treated IDD rats, sh-LINC00284 treatment notably alleviated weak MRI signal intensity of the disc puncture, whereas MRI signal decreased significantly (Fig. 4C and D).

The histological structure of IVD was observed using H&E and safranin-O staining. On day 28, the sh-NC group showed

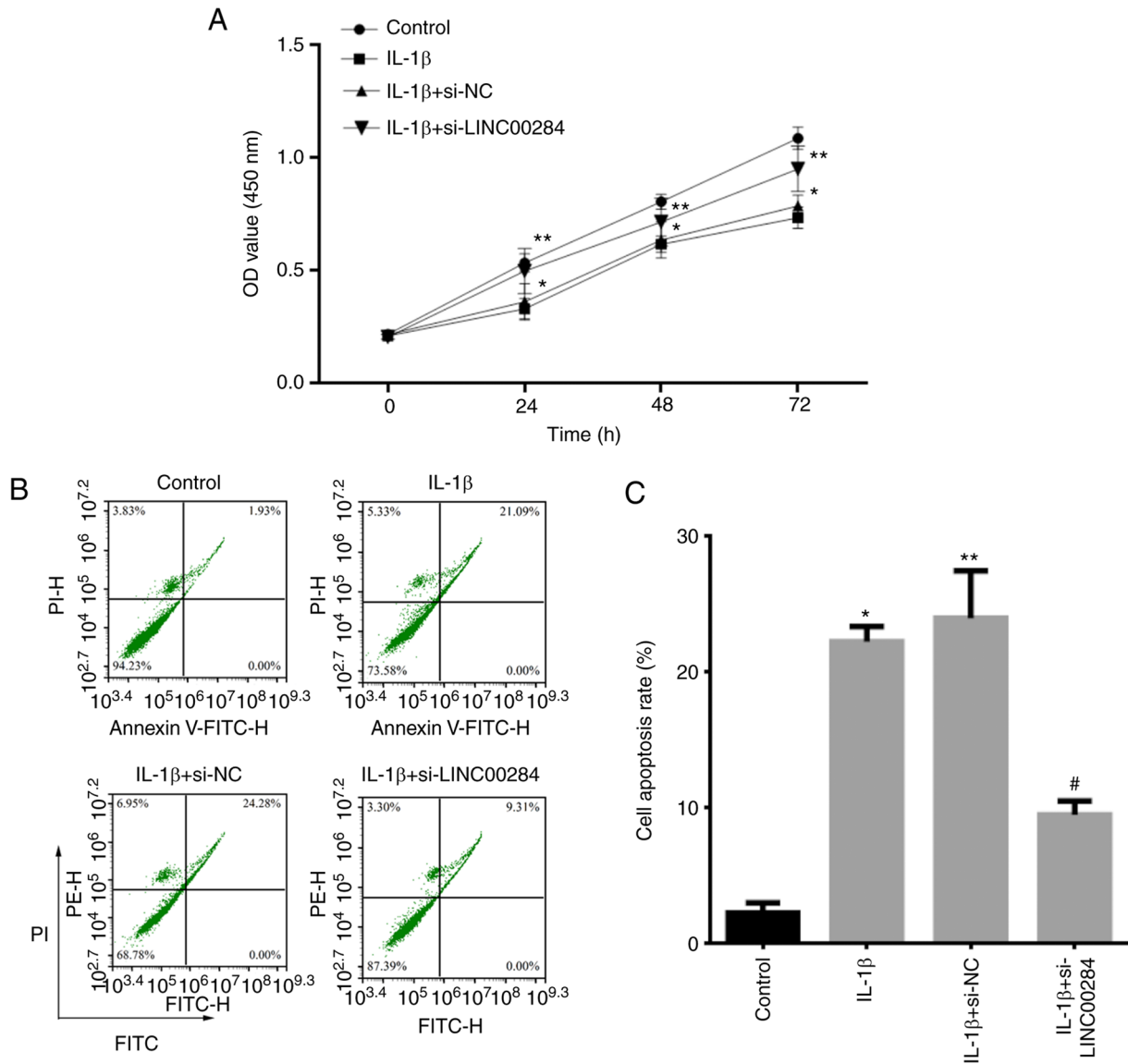


Figure 3. Proliferation and apoptosis of IL-1 $\beta$ -induced NP cells is affected by LINC00284 knockdown. (A) Proliferation of IL-1 $\beta$ -induced NP cells promoted by si-LINC00284 was measured using Cell Counting Kit-8 assay. (B) Cell apoptosis was detected using Annexin V/PI staining and flow cytometry analysis. (C) Apoptotic rate of IL-1 $\beta$ -induced NP cells was inhibited by si-LINC00284. \* $P < 0.05$  vs. Control; \*\* $P < 0.05$  vs. IL-1 $\beta$ ; # $P < 0.05$  vs. IL-1 $\beta$  + si-NC. si, small interfering; NP, nucleus pulposus; OD, optical density; NC, negative control.

a notable decrease in number of NP cells and destruction of AF lamella compared with sham (Fig. 4E and F). Compared with IDD rats treated with sh-NC, sh-LINC00284 treatment preserved the complete structure of the NP and AF; histological grade of the sh-LINC00284 group on days 7, 14 and 28 increased by 13.1, 15.5 and 17.5% respectively (Fig. 4G). The results indicated that LINC00240 may be a therapeutic target of IDD.

*LINC00284 is the direct target of miR-205-3p.* To investigate whether LINC00284 affected ECM degradation in IL-1 $\beta$ -induced NP cells, the target ncRNA of miR-205-3p was predicted using DIANA-LncBase V2 (Fig. 5A) and wt and mut binding sites between LINC00284 and miR-205-3p were established. The luciferase activity of wt-LINC00284 and miR-205-3p mimic co-transfected cells was significantly decreased compared with cells co-transfected with mi-NC transfected cells and mut-LINC00284 and miR-205-3p mimic

co-transfected cells (Fig. 5B). These results indicated that LINC00284 was the direct target of miR-205-3p.

*LINC00284 is regulated by miR-205-3p in NP cells and their expression is correlated in IDD tissue.* To validate the interaction between LINC00284 and miR-205-3p, the effect of transfection of miR-205-3p mimics on expression of LINC00284 was evaluated in NP cells. IL-1 $\beta$  induced upregulation of LINC00284 compared with control but miR-205-3p mimic transfection significantly inhibited LINC00284 expression levels compared with mi-NC-treated cells (Fig. 5C). RT-qPCR showed that miR-205-3p levels were significantly downregulated in 30 IDD compared with 30 spinal cord injury tissue samples (Fig. 5D). Moreover, there was a significant negative correlation between LINC00284 and miR-205-3p expression in 30 IDD tissue samples (Fig. 5E). The results indicated that miR-205-3p was low-expressed and was negative correlated with LINC00240 expression in NP tissues of IDD patients.

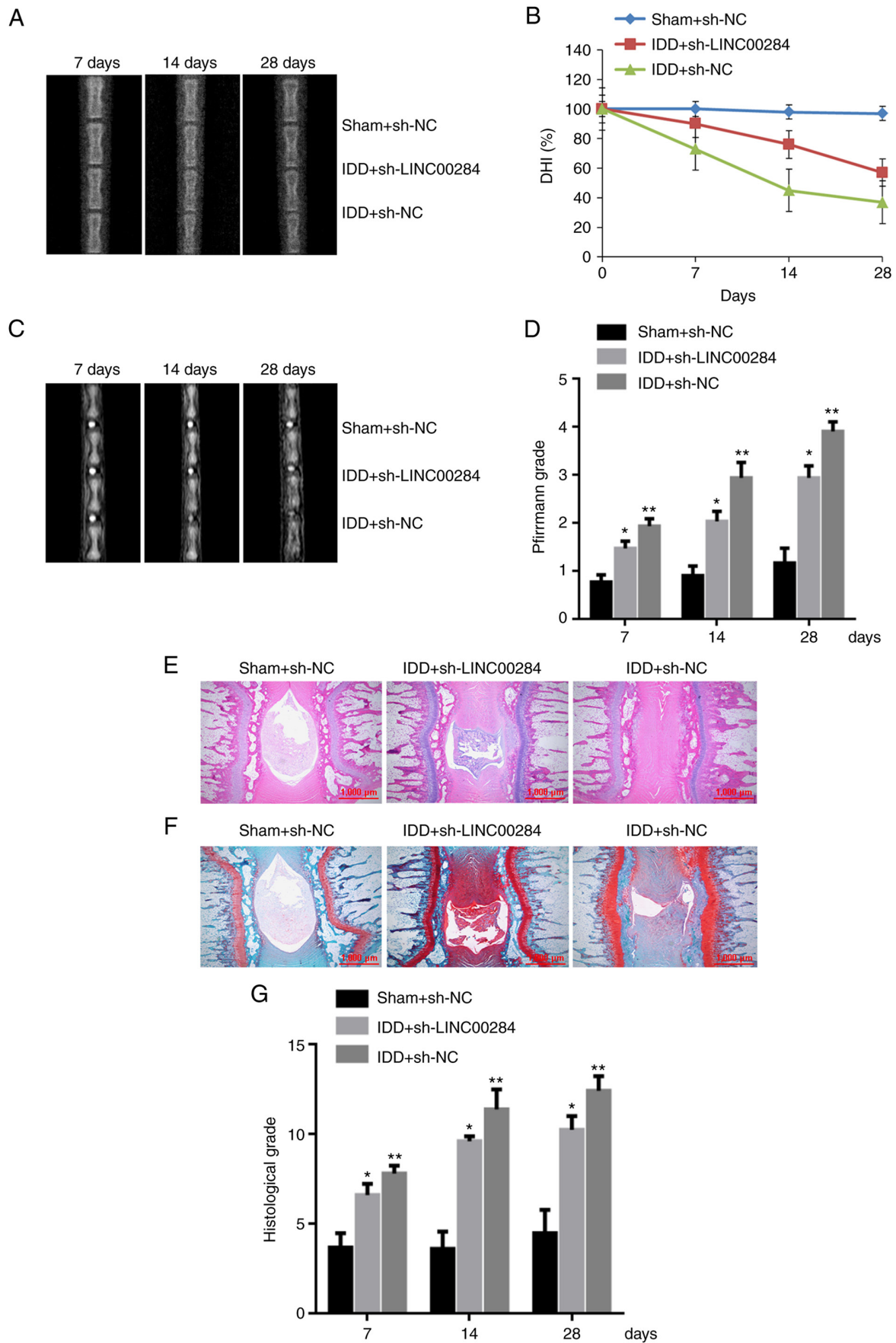


Figure 4. Downregulation of LINC00284 improves puncture-induced IDD *in vivo*. (A) Representative radiographs of coccygeal vertebrae, (B) DHI change, (C) representative MRI scans of coccygeal vertebrae and (D) changes in Pfirrmann grade on days 7, 14 and 28 after initial puncture. (E) Hematoxylin and eosin staining of whole-tail disc sections from IDD rats on day 28 post-initial puncture. (F) Safranin-O staining of whole-tail disc sections from IDD rats. (G) Histological grade on days 7, 14 and 28 days post-initial puncture. Scale bar, 1,000  $\mu$ m. \* $P < 0.05$  vs. sham + sh-NC; \*\* $P < 0.05$  vs. IDD + sh-NC. IDD, intervertebral disc degeneration; DHI, disc height index; sh, short hairpin; NC, negative control.

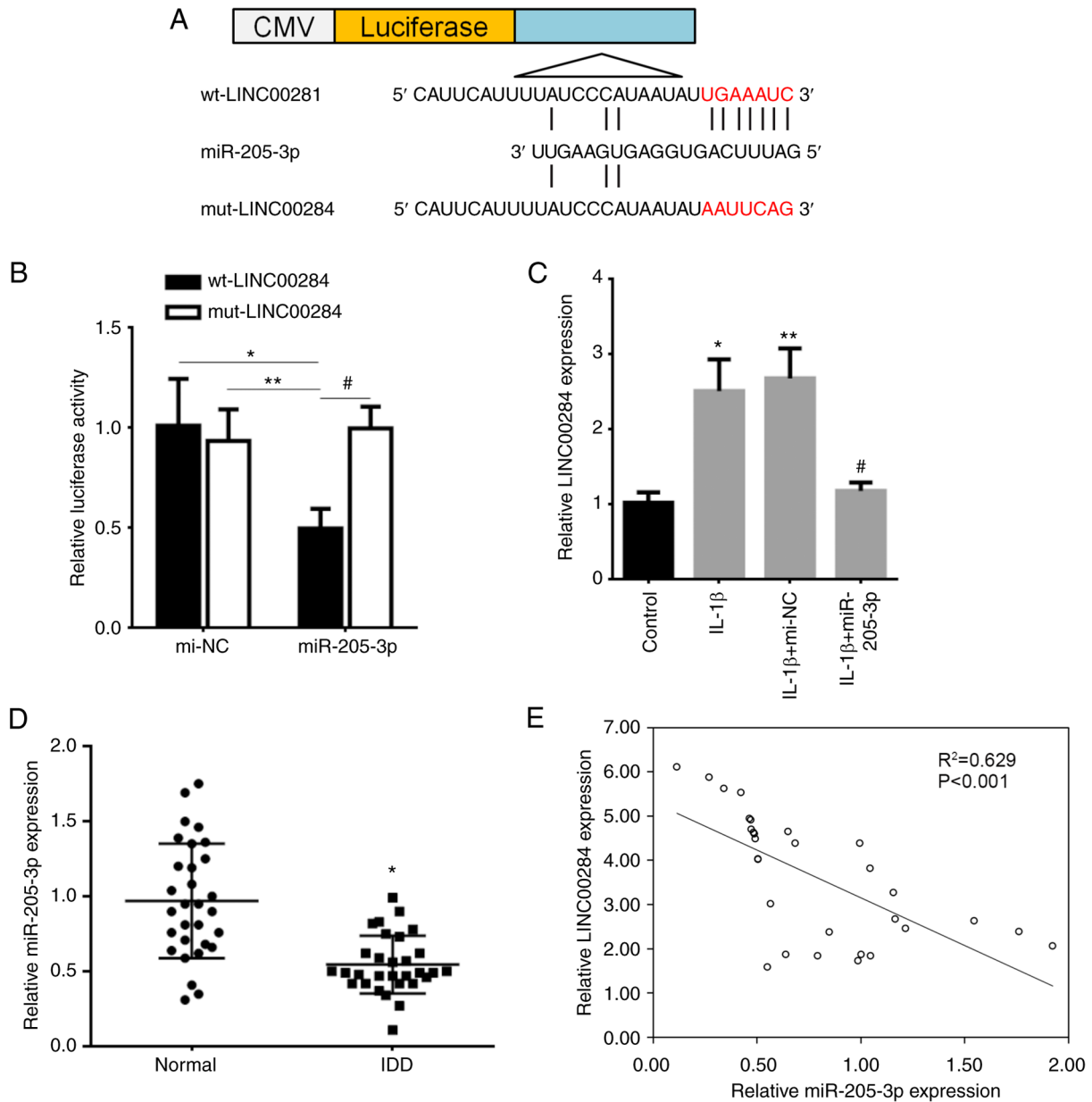


Figure 5. Correlation between LINC00284 and miR-205-3p expression in IDD. (A) Binding site (red) between LINC00284 and miR-205-3p was predicted and assessed using dual luciferase reporter vectors containing wt-LINC00284 or mut-LINC00284. (B) Vectors were co-transfected into 293T cells with miR-205-3p mimics, then luciferase activity was detected using a dual-luciferase reporter assay. \* $P<0.05$  vs. mi-NC and wt-LINC00284 co-transfected cells, \*\* $P<0.05$  vs. mi-NC and mut-LINC00284 co-transfected cells, # $P<0.05$  vs. miR-205-3p and mut-LINC00284 co-transfected cells. (C) Expression levels of LINC00284 were downregulated by miR-205-3p in IL-1 $\beta$ -induced NP cells. \* $P<0.05$  vs. control; \*\* $P<0.05$  vs. IL-1 $\beta$ ; # $P<0.05$  vs. IL-1 $\beta$  + mi-NC. (D) Expression levels of LINC00284 in 30 IDD and 30 normal tissue samples, \* $P<0.001$  vs. normal tissue samples. (E) Negative correlation between miR-205-3p and LINC00284 expression in IDD tissue. IDD, intervertebral disc degeneration; mi-NC, miR-negative control; CMV, cytomegalovirus; wt, wild-type; mut, mutated; miR, microRNA.

*miR-205-3p-mediated LINC00284 downregulation promotes IL-1 $\beta$ -induced proliferation and inhibits apoptosis of NP cells and promotes ECM synthesis.* To confirm the effect of miR-205-3p-mediated regulation of LINC00284 on proliferation, apoptosis and ECM synthesis, miR-205-3p mimics were transfected into IL-1 $\beta$ -induced NP cells. Compared with mi-NC-treated cells, proliferation was increased by miR-205-3p overexpression (Fig. 6A). Furthermore, the cell apoptosis was promoted in IL-1 $\beta$  treated NP cells and mi-NC treated IL-1 $\beta$ -induced NP cells, but a suppressive effect on cell apoptosis was observed following miR-205-3p upregulation (Fig. 6B and C). Western blot analysis showed that, compared with control (untreated NP cells), MMP-3 protein levels were upregulated but aggrecan and

collagen II protein levels were downregulated in IL-1 $\beta$  treated NP cells and mi-NC treated IL-1 $\beta$ -induced NP cells. Compared with mi-NC treated IL-1 $\beta$ -induced NP cells, MMP-3 protein levels were downregulated by miR-205-3p, whereas aggrecan and collagen II protein levels were upregulated in IL-1 $\beta$ -induced NP cells (Fig. 6D-G). The results indicated that LINC00284 can be inhibited by miR-205-3p in IDD through the promotion of NP cell proliferation and ECM synthesis.

*LINC00284 knockdown promotes IL-1 $\beta$ -induced ECM synthesis in NP cells via Wnt/ $\beta$ -catenin signaling.* Wnt/ $\beta$ -catenin signaling has been demonstrated to regulate inflammation in the musculoskeletal system and  $\beta$ -catenin is

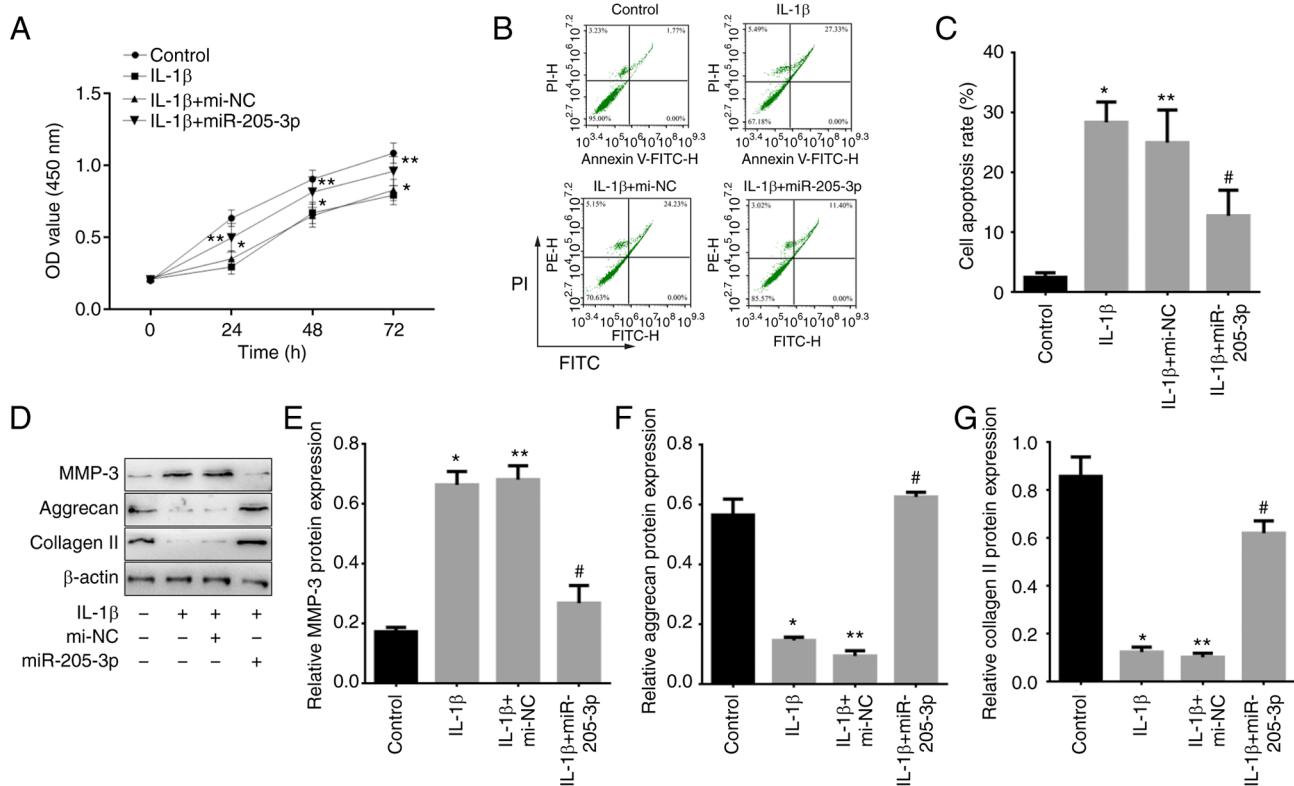


Figure 6. Proliferation and apoptosis of IL-1 $\beta$ -induced NP cells and ECM synthesis following miR-205-3p transfection. (A) Proliferation of NP cells following IL-1 $\beta$  treatment and/or miR-205-3p transfection was determined via Cell Counting Kit-8 assay. (B) NP cells were analyzed following IL-1 $\beta$  treatment and/or miR-205-3p transfection using Annexin V-FITC/PI and flow cytometry analysis and (C) apoptotic rate was determined. (D) The blots of MMP-3, aggrecan and collagen II protein expression measured by western blot assay, expression of (E) MMP-3 and ECM markers (F) aggrecan and (G) collagen II following miR-205-3p transfection in IL-1 $\beta$ -induced NP cells. \* $P$ <0.05 vs. Control; \*\* $P$ <0.05 vs. IL-1 $\beta$ ; # $P$ <0.05 vs. IL-1 $\beta$  + mi-NC. NP, nucleus pulposus; ECM, extracellular matrix; mi-NC, miR-negative control; miR, microRNA; MMP-3, matrix metalloproteinase-3; OD, optical density.

controlled by non-genomic mechanisms (26,27). To investigate if this signaling pathway participated in LINC00284-mediated rescue of ECM degradation via competitively binding with miR-205-3p, si-LINC00284 and/or miR-205-3p mimics were co-transfected into IL-1 $\beta$ -induced NP cells. Compared with control, the protein levels of MMP-3, Wnt1 and  $\beta$ -catenin were increased but aggrecan and collagen II were decreased in IL-1 $\beta$  treated NP cells and si-NC treated IL-1 $\beta$ -induced NP cells. Compared with si-NC treated IL-1 $\beta$ -induced cells, si-LINC00284 resulted in decreased MMP-3, Wnt1 and  $\beta$ -catenin but an increase in aggrecan and collagen II protein levels. Co-transfection of si-LINC00284 with miR-205-3p reversed this effect (Fig. 7). These results indicated that the effect of LINC00284 on promoting ECM degradation may partially be mediated via the Wnt/ $\beta$ -catenin signaling pathway.

## Discussion

IDD is characterized by disorders in ECM metabolism, abnormal proliferation and increased expression of numerous inflammatory factors including IL-1 $\beta$ , IL-8 and TNF- $\alpha$  in NP cells (41). Although multiple factors including SIRT7, NTRK2, and CHI3L1 (42) contribute to etiology of IDD, the molecular mechanism underlying its development remains unclear. An increasing body of evidence has indicated that ncRNAs, including lncRNAs and miRNAs, serve key roles in IDD (13). lncRNA00641 regulates autophagy and IVD degeneration by

acting as a ceRNA of miR-153-3p under stress induced by nutritional deprivation (43). lncRNA taurine upregulated 1 promotes NP cell apoptosis by regulating the miR-26a/high mobility group 1 axis (44). In the present study, LINC00284 expression was significantly upregulated in IDD tissue and IL-1 $\beta$ -induced NP cells. LINC00284 knockdown promoted proliferation and decreased apoptosis of IL-1 $\beta$ -induced NP cells; expression of aggrecan and collagen II, ECM markers of disc degeneration, was also upregulated.

IVD consists of an outer fibrous layer, AF, an inner gelatinous core rich in proteoglycans and NP (45). NP cells serve key roles in maintaining IVD integrity (46); abnormal proliferation of NP cells results in the appearance of cell clusters, which are the primary feature of IVD degeneration (47). Consistent with the results that LINC00284 promotes cell proliferation in ovarian cancer (48), in the present study, LINC00284 inhibited proliferation and promoted NP cell apoptosis. Furthermore, knockdown of LINC00284 using a targeting siRNA resulted in promotion of proliferation and inhibition of apoptosis; *in vivo* analysis showed that LINC00284 knockdown attenuated IDD in the rat model. These results suggested that LINC00284 may be a potent activator of IDD progression. Additionally, the effect of LINC00284 on needle puncture IDD model rats was assessed; IDD rats with LINC00284 knockdown showed a decrease in MRI grade and increase in histological grade. The *in vivo* experiments confirmed results of *in vitro* analysis and suggested that LINC00284 promoted IDD progression.

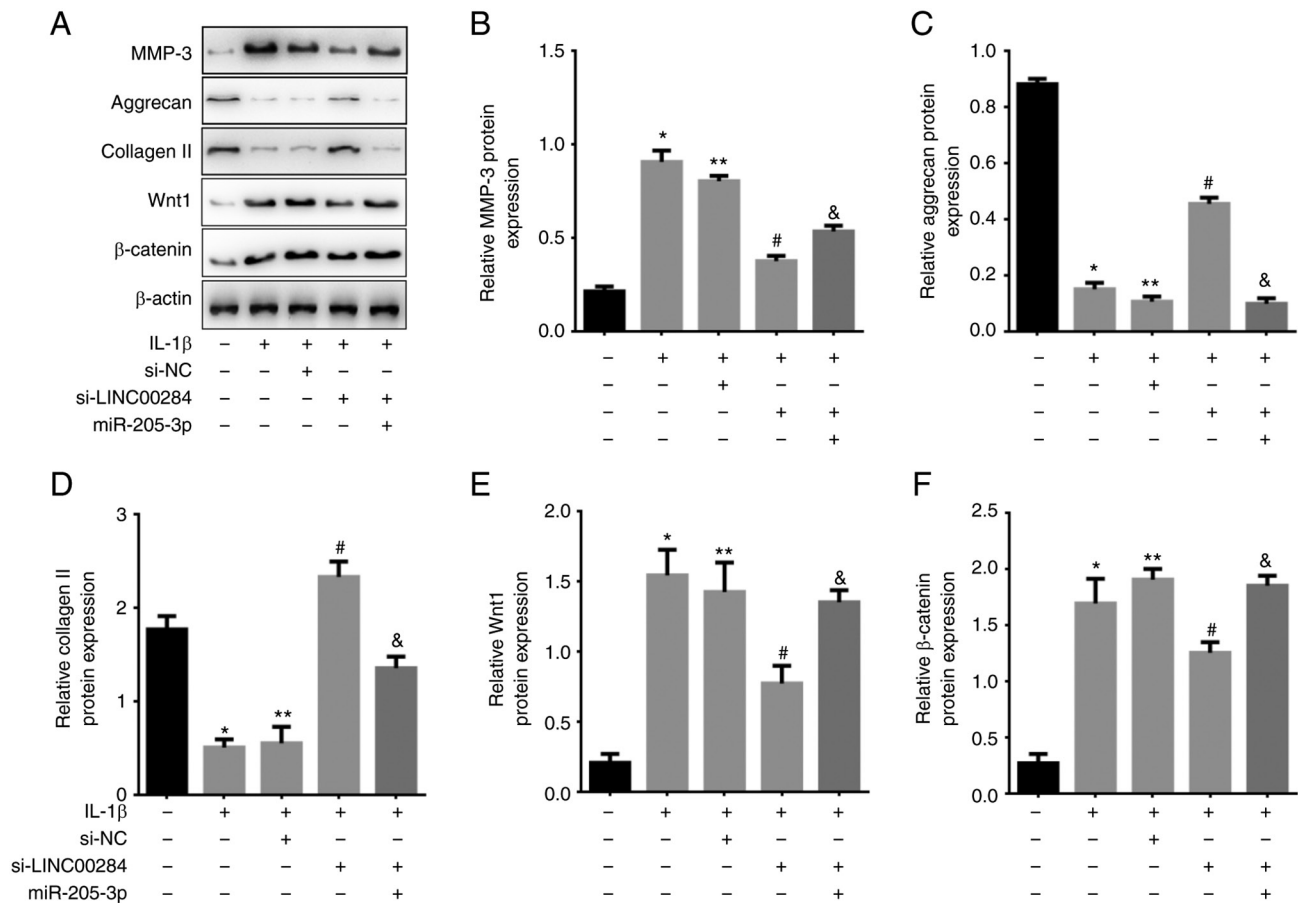


Figure 7. LINC00284 regulates ECM synthesis in IL-1 $\beta$ -induced NP cells via the miR-205-3p/Wnt/ $\beta$ -catenin signaling pathway axis. (A) Expression of MMP-3, ECM markers and Wnt/ $\beta$ -catenin pathway markers following si-LINC00284 and/or miR-205-3p transfection in IL-1 $\beta$ -induced NP cells, as determined by western blotting. (B) MMP-3, (C) aggrecan, (D) collagen II, (E) Wnt1 and (F)  $\beta$ -catenin protein levels following si-LINC00284 and/or miR-205-3p transfection. \* $P$ <0.05 vs. Control; \*\* $P$ <0.05 vs. IL-1 $\beta$ ; # $P$ <0.05 vs. si-NC; & $P$ <0.05 vs. si-LINC00284. ECM, extracellular matrix; NP, nucleus pulposus; MMP-3, matrix metalloproteinase-3; si, small interfering; NC, negative control; miR, microRNA.

lncRNAs serve as sponges as ceRNAs by targeting miRNAs to participate in regulation of pathophysiological processes, including in IDD. lncRNA HLA complex group 18 serves as an endogenous sponge to downregulate miR-146a-5p expression, thus suppressing proliferation of NP cells (49); lncRNA RNA component of mitochondrial RNA processing endoribonuclease interacts with miR-206 to induce upregulation of miR-206, thus promoting proliferation of NP cells (50). In papillary thyroid cancer (PTC), Zhao *et al* (51) demonstrated LINC00284 may serve as a ceRNA to interact with miR-205 and E2F and increased expression of LINC00284 was positively correlated with prognosis of PTC. Consistently, in the present study, it was predicted that miR-205-3p may possess a binding site for LINC00284 using DIANA-LncBase V2; it was confirmed that miR-205-3p inhibited LINC00284 expression via base-pair complementary binding. miR-205-3p expression was upregulated in IDD tissue and expression levels of LINC00284 and miR-205-3p were negatively correlated. Furthermore, the promotive effect of LINC00284 knockdown on IL-1 $\beta$ -induced cell proliferation and ECM synthesis was partially reversed by miR-205-3p, suggesting that LINC00284 may act as a ceRNA to regulate ECM synthesis by sponging miR-205-3p.

The Wnt/ $\beta$ -catenin signaling pathway serves a regulatory role in IDD (52). Hiyama *et al* (53) found that activation of the

Wnt/ $\beta$ -catenin signaling pathway promotes IDD cell senescence and apoptosis, consistent with the results of the present study, which showed that LINC00284 knockdown inhibited the Wnt/ $\beta$ -catenin signaling pathway, as well as the rate of proliferation and apoptosis. These results suggested that LINC00284 may serve a key role in the progression of IDD via activation of the Wnt/ $\beta$ -catenin signaling pathway.

In conclusion, LINC00284 served as a ceRNA to activate the Wnt/ $\beta$ -catenin signaling pathway by sponging miR-205-3p, resulting in inhibition of cell proliferation in the NP as well as ECM synthesis in IDD. Thus, LINC00284 knockdown to rescue miR-205-3p expression may be a promising strategy to treat IDD.

#### Acknowledgements

Not applicable.

#### Funding

The present study was supported by Jiangsu Health and Family Planning Commission, China (grant no. Y2018099) and Science Foundation of Nantong City, Jiangsu Province, China (grant no. JCZ20121).

### Availability of data and materials

All the data generated or analyzed during the present study are included in this published article.

### Authors' contributions

MZ and YS conceived and designed the study. XY, HX, ZW, BW and XL performed the experiments. YZ collected and analyzed tissue samples. MZ, XY and YS acquired, analyzed and interpreted the data. HX, ZW, BW and XL reviewed the manuscript. MZ drafted and revised the manuscript. All authors have read and approved the final manuscript. MZ and YS confirm the authenticity of all the raw data.

### Ethics approval and consent to participate

The present study was approved and supervised by the Ethics Committee of Shanghai Changzheng Hospital, Second Military Medical University. Written informed consent was provided by all subjects. Animal experiments were approved by the Institutional Animal Care and Use Committee of Shanghai Changzheng Hospital, Second Military Medical University. Great effort was made to minimize the number of animals used and their respective suffering.

### Patient consent for publication

Not applicable.

### Competing interests

The authors declare that they have no competing interests.

### References

- Liu C, Yang M, Liu L, Zhang Y, Zhu Q, Huang C, Wang H, Zhang Y, Li H, Li C, *et al*: Molecular basis of degenerative spinal disorders from a proteomic perspective (Review). *Mol Med Rep* 21: 9-19, 2020.
- Setton LA and Chen J: Mechanobiology of the intervertebral disc and relevance to disc degeneration. *J Bone Joint Surg Am* 88 (Suppl 2): S52-S57, 2006.
- Balagué F, Mannion AF, Pellisé F and Cedraschi C: Non-specific low back pain. *Lancet* 379: 482-891, 2012.
- Battié MC, Videman T and Parent E: Lumbar disc degeneration: Epidemiology and genetic influences. *Spine (Phila Pa 1976)* 29: 2679-2690, 2004.
- Battié MC and Videman T: Lumbar disc degeneration: Epidemiology and genetics. *J Bone Joint Surg Am* 88 (Suppl 2): S3-S9, 2006.
- Feng H, Danfelter M, Strömquist B and Heinegård D: Extracellular matrix in disc degeneration. *J Bone Joint Surg Am* 88 (Suppl 2): S25-S29, 2006.
- Roberts S, Caterson B, Menage J, Evans EH, Jaffray DC and Eisenstein SM: Matrix metalloproteinases and aggrecanase: Their role in disorders of the human intervertebral disc. *Spine (Phila Pa 1976)* 25: 3005-3013, 2000.
- Wang SZ, Chang Q, Lu J and Wang C: Growth factors and platelet-rich plasma: Promising biological strategies for early intervertebral disc degeneration. *Int Orthop* 39: 927-934, 2015.
- Richardson SM, Kalamegam G, Pushparaj PN, Matta C, Memic A, Khademhosseini A, Mobasheri R, Poletti FL, Hoyland JA and Mobasheri A: Mesenchymal stem cells in regenerative medicine: Focus on articular cartilage and intervertebral disc regeneration. *Methods* 99: 69-80, 2016.
- Liu H, Pan H, Yang H, Wang J, Zhang K, Li X, Wang H, Ding W, Li B and Zheng Z: LIM mineralization protein-1 suppresses TNF- $\alpha$  induced intervertebral disc degeneration by maintaining nucleus pulposus extracellular matrix production and inhibiting matrix metalloproteinases expression. *J Orthop Res* 33: 294-303, 2015.
- Bach FC, Zhang Y, Miranda-Bedate A, Verdonshot LC, Bergknot N, Creemers LB, Ito K, Sakai D, Chan D, Meij BP and Tryfonidou MA: Increased caveolin-1 in intervertebral disc degeneration facilitates repair. *Arthritis Res Ther* 18: 59, 2016.
- Fujita K, Ando T, Ohba T, Wako M, Sato N, Nakamura Y, Ohnuma Y, Hara Y, Kato R, Nakao A, *et al*: Age-related expression of MCP-1 and MMP-3 in mouse intervertebral disc in relation to TWEAK and TNF- $\alpha$  stimulation. *J Orthop Res* 30: 599-605, 2012.
- Chen WK, Yu XH, Yang W, Wang C, He WS, Yan YG, Zhang J and Wang WJ: lncRNAs: Novel players in intervertebral disc degeneration and osteoarthritis. *Cell Prolif* 50: e12313, 2017.
- Chen Y, Ni H, Zhao Y, Chen K, Li M, Li C, Zhu X and Fu Q: Potential role of lncRNAs in contributing to pathogenesis of intervertebral disc degeneration based on microarray data. *Med Sci Monit* 21: 3449-3458, 2015.
- Wan ZY, Song F, Sun Z, Chen YF, Zhang WL, Samartzis D, Ma CJ, Che L, Liu X, Ali MA, *et al*: Aberrantly expressed long noncoding RNAs in human intervertebral disc degeneration: A microarray related study. *Arthritis Res Ther* 16: 465, 2014.
- Cui S, Liu Z, Tang B, Wang Z and Li B: lncRNA MAGI2-AS3 is down-regulated in intervertebral disc degeneration and participates in the regulation of FasL expression in nucleus pulposus cells. *BMC Musculoskelet Disord* 21: 149, 2020.
- Zhang Z, Huo Y, Zhou Z, Zhang P and Hu J: Role of lncRNA PART1 in intervertebral disc degeneration and associated underlying mechanism. *Exp Ther Med* 21: 131, 2021.
- Yildiz-Arslan S, Coon JS, Hope TJ and Kim JJ: Transcriptional profiling of human endocervical tissues reveals distinct gene expression in the follicular and luteal phases of the menstrual cycle. *Biol Reprod* 94: 138, 2016.
- Xing C, Cai Z, Gong J, Zhou J, Xu J and Guo F: Identification of potential biomarkers involved in gastric cancer through integrated analysis of non-coding RNA associated competing endogenous RNAs network. *Clin Lab* 64: 1661-1669, 2018.
- Zhang L and Guo Y: Silencing circular RNA-ZNF652 represses proliferation and EMT process of renal carcinoma cells via raising miR-205. *Artif Cells Nanomed Biotechnol* 48: 648-655, 2020.
- Song Y, Guo NH and Zheng JF: lncRNA-MALAT1 regulates proliferation and apoptosis of acute lymphoblastic leukemia cells via miR-205-PTK7 pathway. *Pathol Int* 70: 724-732, 2020.
- Chen B, Li Y, Liu Y and Xu Z: circLRP6 regulates high glucose-induced proliferation, oxidative stress, ECM accumulation, and inflammation in mesangial cells. *J Cell Physiol* 234: 21249-21259, 2019.
- Frank S, Peters MA, Wehmeyer C, Strietholt S, Koers-Wunrau C, Bertrand J, Heitzmann M, Hillmann A, Sherwood J, Seyfert C, *et al*: Regulation of matrixmetalloproteinase-3 and matrixmetalloproteinase-13 by SUMO-2/3 through the transcription factor NF- $\kappa$ B. *Ann Rheum Dis* 72: 1874-1881, 2013.
- Hiyama A, Gogate SS, Gajghate S, Mochida J, Shapiro IM and Risbud MV: BMP-2 and TGF- $\beta$  stimulate expression of beta1,3-glucuronosyl transferase 1 (GlcAT-1) in nucleus pulposus cells through AP1, TonEBP, and Sp1: Role of MAPKs. *J Bone Miner Res* 25: 1179-1190, 2010.
- Mäkitie RE, Niinimäki T, Nieminen MT, Schalin-Jäntti C, Niinimäki J and Mäkitie O: Impaired WNT signaling and the spine-Heterozygous WNT1 mutation causes severe age-related spinal pathology. *Bone* 101: 3-9, 2017.
- Ge XP, Gan YH, Zhang CG, Zhou CY, Ma KT, Meng JH and Ma XC: Requirement of the NF- $\kappa$ B pathway for induction of Wnt-5A by interleukin-1 $\beta$  in condylar chondrocytes of the temporomandibular joint: Functional crosstalk between the Wnt-5A and NF- $\kappa$ B signaling pathways. *Osteoarthritis Cartilage* 19: 111-117, 2011.
- Reya T and Clevers H: Wnt signalling in stem cells and cancer. *Nature* 434: 843-850, 2005.
- Söderholm S and Cantù C: The WNT/ $\beta$ -catenin dependent transcription: A tissue-specific business. *WIREs Mech Dis* 13: e1511, 2021.
- Rauner M, Stein N, Winzer M, Goetsch C, Zwerina J, Schett G, Distler JH, Albers J, Schulze J, Schinke T, *et al*: WNT5A is induced by inflammatory mediators in bone marrow stromal cells and regulates cytokine and chemokine production. *J Bone Miner Res* 27: 575-585, 2012.

30. Nakamura Y, Nawata M and Wakitani S: Expression profiles and functional analyses of Wnt-related genes in human joint disorders. *Am J Pathol* 167: 97-105, 2005.
31. World Medical Association: World medical association declaration of Helsinki: Ethical principles for medical research involving human subjects. *JAMA* 310: 2191-2194, 2013.
32. Livak KJ and Schmittgen TD: Analysis of relative gene expression data using real-time quantitative PCR and the 2(-Delta Delta C(T)) method. *Methods* 25: 402-408, 2001.
33. Paraskevopoulou MD, Vlachos IS, Karagkouni D, Georgakilas G, Kanellos I, Vergoulis T, Zagganas K, Tsanakas P, Floros E, Dalamagas T and Hatzigeorgiou AG: DIANA-LncBase v2: Indexing microRNA targets on non-coding transcripts. *Nucleic Acids Res* 44: D231-D238, 2016.
34. Li Z, Liu H, Yang H, Wang J, Wang H, Zhang K, Ding W and Zheng Z: Both expression of cytokines and posterior annulus fibrosus rupture are essential for pain behavior changes induced by degenerative intervertebral disc: An experimental study in rats. *J Orthop Res* 32: 262-272, 2014.
35. Council N: Guide for the care and use of laboratory animals: Eighth edition. Publication 327: pp963-965, 2010.
36. Zhang J, Li Z, Chen F, Liu H, Wang H, Li X, Liu X, Wang J and Zheng Z: TGF- $\beta$ 1 suppresses CCL3/4 expression through the ERK signaling pathway and inhibits intervertebral disc degeneration and inflammation-related pain in a rat model. *Exp Mol Med* 49: e379, 2017.
37. Miyagi M, Ishikawa T, Kamoda H, Suzuki M, Sakuma Y, Orita S, Oikawa Y, Aoki Y, Toyone T, Takahashi K, *et al*: Assessment of pain behavior in a rat model of intervertebral disc injury using the CatWalk gait analysis system. *Spine (Phila Pa 1976)* 38: 1459-1465, 2013.
38. Han B, Zhu K, Li FC, Xiao YX, Feng J, Shi ZL, Lin M, Wang J and Chen QX: A simple disc degeneration model induced by percutaneous needle puncture in the rat tail. *Spine (Phila Pa 1976)* 33: 1925-1934, 2008.
39. Pfirrmann CW, Metzendorf A, Zanetti M, Hodler J and Boos N: Magnetic resonance classification of lumbar intervertebral disc degeneration. *Spine (Phila Pa 1976)* 26: 1873-1878, 2001.
40. Masuda K, Aota Y, Muehleman C, Imai Y, Okuma M, Thonar EJ, Andersson GB and An HS: A novel rabbit model of mild, reproducible disc degeneration by an annulus needle puncture: Correlation between the degree of disc injury and radiologic and histological appearances of disc degeneration. *Spine (Phila Pa 1976)* 30: 5-14, 2005.
41. Liu ZM, Lu CC, Shen PC, Chou SH, Shih CL, Chen JC and Tien YC: Suramin attenuates intervertebral disc degeneration by inhibiting NF- $\kappa$ B signalling pathway. *Bone Joint Res* 10: 498-513, 2021.
42. Li H, Li W, Zhang L, He J, Tang L, Li Z, Chen F, Fan Q and Wei J: Comprehensive network analysis identified SIRT7, NTRK2, and CHI3L1 as new potential markers for intervertebral disc degeneration. *J Oncol* 2022: 4407541, 2022.
43. Wang XB, Wang H, Long HQ, Li DY and Zheng X: LINC00641 regulates autophagy and intervertebral disc degeneration by acting as a competitive endogenous RNA of miR-153-3p under nutrition deprivation stress. *J Cell Physiol* 234: 7115-7127, 2019.
44. Tang N, Dong Y, Xiao T and Zhao H: LncRNA TUG1 promotes the intervertebral disc degeneration and nucleus pulposus cell apoptosis through modulating miR-26a/HMGB1 axis and regulating NF- $\kappa$ B activation. *Am J Transl Res* 12: 5449-5464, 2020.
45. Kirnaz S, Singh S, Capadona C, Lintz M, Goldberg JL, McGrath LB Jr, Medary B, Sommer F, Bonassar LJ and Härtl R: Innovative biological treatment methods for degenerative disc disease. *World Neurosurg* 157: 282-299, 2022.
46. Johnson WE, Eisenstein SM and Roberts S: Cell cluster formation in degenerate lumbar intervertebral discs is associated with increased disc cell proliferation. *Connect Tissue Res* 42: 197-207, 2001.
47. Daisuke T and Horton P: Inference of scale-free networks from gene expression time series. *J Bioinform Comput Biol* 4: 503-514, 2006.
48. Ruan Z and Zhao D: Long intergenic noncoding RNA LINC00284 knockdown reduces angiogenesis in ovarian cancer cells via up-regulation of MEST through NF- $\kappa$ B1. *FASEB J* 33: 12047-12059, 2019.
49. Xi Y, Jiang T, Wang W, Yu J, Wang Y, Wu X and He Y: Long non-coding HCG18 promotes intervertebral disc degeneration by sponging miR-146a-5p and regulating TRAF6 expression. *Sci Rep* 7: 13234, 2017.
50. Wang X, Peng L, Gong X, Zhang X, Sun R and Du J: LncRNA-RMRP promotes nucleus pulposus cell proliferation through regulating miR-206 expression. *J Cell Mol Med* 22: 5468-5476, 2018.
51. Zhao Y, Wang H, Wu C, Yan M, Wu H, Wang J, Yang X and Shao Q: Construction and investigation of lncRNA-associated ceRNA regulatory network in papillary thyroid cancer. *Oncol Rep* 39: 1197-1206, 2018.
52. Xie H, Jing Y, Xia J, Wang X, You C and Yan J: Aquaporin 3 protects against lumbar intervertebral disc degeneration via the Wnt/ $\beta$ -catenin pathway. *Int J Mol Med* 37: 859-864, 2016.
53. Hiyama A, Sakai D, Risbud MV, Tanaka M, Arai F, Abe K and Mochida J: Enhancement of intervertebral disc cell senescence by WNT/ $\beta$ -catenin signaling-induced matrix metalloproteinase expression. *Arthritis Rheum* 62: 3036-3047, 2010.



This work is licensed under a Creative Commons Attribution-NonCommercial-NoDerivatives 4.0 International (CC BY-NC-ND 4.0) License.